

THE SCALAR AND PSEUDOSCALAR HIDDEN-CHARM TETRAQUARK STATES WITH QCD SUM RULES

Zun-Yan Di^{1,2}, Zhi-Gang Wang^{1*}

¹ Department of Physics, North China Electric Power University, Baoding 071003, P. R. China

² School of Nuclear Science and Engineering, North China Electric Power University, Beijing 102206, P. R. China

Abstract

Based on the diquark configuration, we construct the diquark-antidiquark interpolating tetraquark currents with $J^{PC} = 1^{-\pm}$ and $1^{+\pm}$, which can couple to the scalar and pseudoscalar tetraquark states respectively, since they are not conserved currents. Then we investigate their two-point correlation functions including the contributions of the vacuum condensates up to dimension-10 and extract the masses and pole residues of the tetraquark states with $J^{PC} = 0^{+\pm}$ and $0^{-\pm}$ through the QCD sum rule approach. The predicted masses can be confronted with the experimental data in the future. Moreover, we briefly discuss the possible decay patterns of the tetraquark states.

PACS number: 12.39.Mk, 12.38.Lg

Key words: Hidden-charm tetraquark state, QCD sum rules

1 Introduction

Since the discovery of the $X(3872)$ resonance by Belle collaboration in 2003 [1], more and more exotic hadrons have been observed and confirmed experimentally, such as the charmonium-like XYZ states [2], hidden-charm pentaquarks [3], etc. These resonances with four or five valence quarks cannot be interpreted as conventional quark-antiquark mesons or three-quark baryons in the quark model [4]. They are new blocks of QCD matter, which provide an important platform to deepen our understanding of the low energy behaviors of QCD.

Facing the large amount of data on the exotic states, the theoretical researchers of high energy physics have proposed several models to explain their nature, such as molecule, multiquark state, hadrocharmonium, hybrids, kinematical effects, etc. In the molecular picture, a tetraquark (pentaquark) state is explained as a hadronic molecule of two mesons (one meson and one baryon) [5, 6]. The multiquark state interpretation is based on the phenomenological diquark picture [7], in which a tetraquark state is assumed to be a diquark-antidiquark object [8-19] and a pentaquark state is a diquark-diquark-antiquark object [20-29], bound by gluonic exchanges. In the hadroquarkonium picture for multi-quark exotics, the heavy-quark pair $Q\bar{Q}$ forms a compact core about which the light $q\bar{q}$ or qqq forms a quantum-mechanical cloud [30, 31]. Here, we simply introduce the above three popular models. For more reviews of the theoretical interpretations, see Ref.[32, 33]. Unfortunately, as so far, no single model naturally accommodates all the observed states. It will be a long way to reveal the nature of the multi-quark candidates completely.

In addition, the observations of these exotic states stimulate the arguments for more possible multi-quark states. In Ref.[34], we have studied the possible scalar hidden-charm $cu\bar{c}\bar{d}$ ($cu\bar{c}\bar{s}$) tetraquark states by constructing the corresponding $C \otimes C$ and $C\gamma_\mu\gamma_5 \otimes \gamma_5\gamma^\mu C$ type scalar interpolating currents. In this article, we investigate the other possible scalar and pseudo-scalar hidden-charm tetraquark states with different structures. Specifically, we construct the $C \otimes \gamma_\mu C$ and $C\gamma_5 \otimes \gamma_5\gamma_\mu C$ type interpolating tetraquark currents with $J^{PC} = 1^{-\pm}$ and $1^{+\pm}$ in the diquark configuration, calculate their two-point correlation functions, and extract the spectral densities for the scalar and pseudoscalar tetraquark states through the tensor analysis method. Then we perform the QCD sum rule analysis and obtain the masses and pole residues of the hidden-charm tetraquark states with $J^{PC} = 0^{+\pm}$ and $0^{-\pm}$.

*E-mail: zgwang@aliyun.com.

This article is organized as follows. In section 2, we construct the vector and axial-vector interpolating tetraquark currents, extract the spectral densities for the scalar and pseudoscalar tetraquark states up to dimension-10 and derive the masses and pole residues of the scalar and pseudoscalar tetraquark states with the QCD sum rules. The numerical results and discussions are performed in section 3. The last section is reserved for our conclusion.

2 QCD sum rules for the $J^{PC} = 0^{+\pm}$ and $0^{-\pm}$ hidden-charm tetraquark states

To begin, we construct the diquark-antidiquark interpolating tetraquark currents with $J^{PC} = 1^{-\pm}$ and $1^{+\pm}$, based on the diquark configuration. The vector and axial-vector interpolating currents are

$$J_{\mu}^{t,a}(x) = \frac{\epsilon^{ijk}\epsilon^{imn}}{\sqrt{2}} \{u^{jT}(x)C c^k(x)\bar{d}^m(x)\gamma_{\mu}C\bar{c}^{nT}(x) + tu^{jT}(x)C\gamma_{\mu}c^k(x)\bar{d}^m(x)C\bar{c}^{nT}(x)\} \quad (1)$$

and

$$J_{\mu}^{t,b}(x) = \frac{\epsilon^{ijk}\epsilon^{imn}}{\sqrt{2}} \{u^{jT}(x)C\gamma_5 c^k(x)\bar{d}^m(x)\gamma_{\mu}C\bar{c}^{nT}(x) + tu^{jT}(x)C\gamma_{\mu}c^k(x)\bar{d}^m(x)\gamma_5 C\bar{c}^{nT}(x)\} \quad (2)$$

respectively, where the i, j, k, m and n are color indexes, the C is the charge conjugation matrix. Under charge conjugation transform \widehat{C} , the currents $J_{\mu}^{t,a/b}(x)$ have the properties,

$$\widehat{C}J_{\mu}^{t,a/b}(x)\widehat{C}^{-1} = \pm J_{\mu}^{t,a/b}(x) |_{u\leftrightarrow d} \quad \text{for } t = \pm, \quad (3)$$

which originate from the charge conjugation properties of the scalar, pseudoscalar and axial-vector diquark states,

$$\begin{aligned} \widehat{C}[\epsilon^{ijk}q^j C\gamma_5 c^k]\widehat{C}^{-1} &= \epsilon^{ijk}\bar{q}^j\gamma_5 C\bar{c}^k, \\ \widehat{C}[\epsilon^{ijk}q^j Cc^k]\widehat{C}^{-1} &= \epsilon^{ijk}\bar{q}^j C\bar{c}^k, \\ \widehat{C}[\epsilon^{ijk}q^j C\gamma_{\mu}c^k]\widehat{C}^{-1} &= \epsilon^{ijk}\bar{q}^j\gamma_{\mu}C\bar{c}^k, \end{aligned} \quad (4)$$

where $q = u, d$. Thus the superscript $t = \pm$ of the interpolating currents $J_{\mu}^{t,a/b}(x)$ can correspond the positive and negative charge conjugations for the vector and axial-vector tetraquark states.

In the following, we compute

$$\begin{aligned} p^{\mu}J_{\mu}^{t,a}(x) &= i\partial^{\mu}J_{\mu}^{t,a}(x) \\ &= -\frac{\epsilon^{ijk}\epsilon^{imn}}{\sqrt{2}}(m_c - m_q) \{u^{jT}(x)C c^k(x)\bar{d}^m(x)C\bar{c}^{nT}(x) \\ &\quad - tu^{jT}(x)C c^k(x)\bar{d}^m(x)C\bar{c}^{nT}(x)\} + \dots, \end{aligned} \quad (5)$$

$$\begin{aligned} p^{\mu}J_{\mu}^{t,b}(x) &= i\partial^{\mu}J_{\mu}^{t,b}(x) \\ &= -\frac{\epsilon^{ijk}\epsilon^{imn}}{\sqrt{2}}(m_c - m_q) \{u^{jT}(x)C\gamma_5 c^k(x)\bar{d}^m(x)C\bar{c}^{nT}(x) \\ &\quad - tu^{jT}(x)C c^k(x)\bar{d}^m(x)\gamma_5 C\bar{c}^{nT}(x)\} + \dots, \end{aligned} \quad (6)$$

where $m_q = m_u = m_d$, the p^{μ} is the momentum of the current, which is equivalent to the sum of the constituent quarks' momenta and can be replaced by the $i\partial^{\mu}$ in momentum space. In Eqs.(5)-(6), the derivative operator acts on all quark fields including $u^{jT}(x)C c^k(x)$ and the relevant terms are

not written out because they are complicated, which can not be simplified by the Dirac equation. From the Eqs.(5)-(6), we can see that the $\partial^\mu J_\mu^{t,a/b}(x) \neq 0$, hence the currents $J_\mu^{t,a/b}(x)$ are not conserved and can couple to the scalar and pseudoscalar tetraquark states, respectively. Besides, the Eqs.(5)-(6) indicate that the superscript $t = \mp$ of the interpolating currents $J_\mu^{t,a/b}(x)$ can correspond the positive and negative charge conjugations for the scalar and pseudoscalar tetraquark states.

The two-point correlation functions of the vector and axial-vector currents are written as

$$\begin{aligned}\Pi_{\mu\nu}^{t,a/b}(p) &= i \int d^4x e^{ip \cdot x} \langle 0 | T \left\{ J_\mu^{t,a/b}(x) J_\nu^{t,a/b \dagger}(0) \right\} | 0 \rangle \\ &= \Pi_1^{t,a/b}(p) \left(-g_{\mu\nu} + \frac{p_\mu p_\nu}{p^2} \right) + \Pi_0^{t,a/b}(p) p_\mu p_\nu.\end{aligned}\quad (7)$$

There are two parts of $\Pi_{\mu\nu}^{t,a/b}(p)$ with different Lorentz structures because the currents $J_\mu^{t,a/b}(x)$ are not conserved currents. $\Pi_1^{t,a/b}(p)$ are related to the vector and axial-vector tetraquark states, while $\Pi_0^{t,a/b}(p)$ are the scalar and pseudoscalar current polarization functions.

At the phenomenological side, we insert a complete set of intermediate hadronic states with the same quantum numbers as the current operators $J_\mu^{t,a/b}(x)$ into the correlation functions $\Pi_{\mu\nu}^{t,a/b}(p)$ to obtain the hadronic representation. After isolating the ground state contributions of the hidden-charm tetraquark states from the pole terms, we get the following results,

$$\Pi_{\mu\nu}^{t,a/b}(p) = \frac{\lambda_{Z_1^{t,a/b}}^2}{M_{Z_1^{t,a/b}}^2 - p^2} \left(-g_{\mu\nu} + \frac{p_\mu p_\nu}{p^2} \right) + \frac{\lambda_{Z_0^{t,a/b}}^2}{M_{Z_0^{t,a/b}}^2 - p^2} p_\mu p_\nu + \dots, \quad (8)$$

where the pole residues $\lambda_{Z_1^{t,a/b}}$ and $\lambda_{Z_0^{t,a/b}}$ are defined by

$$\begin{aligned}\langle 0 | J_\mu^{t,a/b}(0) | Z_1^{t,a/b}(p) \rangle &= \lambda_{Z_1^{t,a/b}} \varepsilon_\mu, \\ \langle 0 | J_\mu^{t,a/b}(0) | Z_0^{t,a/b}(p) \rangle &= \lambda_{Z_0^{t,a/b}} p_\mu,\end{aligned}\quad (9)$$

the $Z_1^{t,a/b}$ and $Z_0^{t,a/b}$ are the ground states of the spin-1 and spin-0 hidden-charm tetraquark states, respectively, and the ε_μ are the polarization vectors of the vector and axialvector tetraquark states. In Refs.[35, 36], the authors have chosen the tensor structure $-g_{\mu\nu} + \frac{p_\mu p_\nu}{p^2}$ for analysis and investigated the corresponding vector and axial-vector tetraquark states $Z_1^{t,a/b}$. In this article, we make Eq.(8) multiplied by the p^μ ,

$$p^\mu \Pi_{\mu\nu}^{t,a/b}(p) = \frac{\lambda_{Z_1^{t,a/b}}^2}{M_{Z_1^{t,a/b}}^2 - p^2} \left(-g_{\mu\nu} p^\mu + \frac{p^\mu p_\mu p_\nu}{p^2} \right) + \frac{\lambda_{Z_0^{t,a/b}}^2}{M_{Z_0^{t,a/b}}^2 - p^2} p_\mu p^\mu p_\nu + \dots, \quad (10)$$

to eliminate contaminations of the vector and axial-vector tetraquark states, and study the remaining scalar and pseudoscalar tetraquark states $Z_0^{t,a/b}$.

Now, we take a short digression to study the contributions of the intermediate meson-loops to the correlation function $\Pi_0^{-,a}(p)$ for the current $J_\mu^{-,a}(x)$ as an example, the current $J_\mu^{-,a}(x)$ has non-vanishing couplings with the scattering states $\eta_c \pi^+$, $J/\psi \rho^+(770)$, $\bar{D}^0 D^+$, etc.

$$\Pi_0^{-,a}(p) = -\frac{\widehat{\lambda}_{Z_0^{-,a}}^2}{p^2 - \widehat{M}_{Z_0^{-,a}}^2 - \Sigma_{\eta_c \pi^+}(p) - \Sigma_{J/\psi \rho^+(770)}(p) - \Sigma_{\bar{D}^0 D^+}(p) + \dots} + \dots, \quad (11)$$

where the $\widehat{\lambda}_{Z_0^{-,a}}$ and $\widehat{M}_{Z_0^{-,a}}$ are bare quantities to absorb the divergences in the self-energies

$\Sigma_{\eta_c\pi^+}(p)$, $\Sigma_{J/\psi\rho^+}(770)(p)$, $\Sigma_{\bar{D}^0D^+}(p)$, etc. The renormalized self-energies contribute a finite imaginary part to modify the dispersion relation,

$$\Pi_0^{-,a}(p) = -\frac{\lambda_{Z_0^{-,a}}^2}{p^2 - M_{Z_0^{-,a}}^2 + i\sqrt{p^2}\Gamma(p^2)} + \dots \quad (12)$$

In previous works, we observed that the effects of the finite widths, such as $\Gamma_{X(4500)} = 92 \pm 21_{-20}^{+21}$ MeV, $\Gamma_{X(4700)} = 120 \pm 31_{-33}^{+42}$ MeV, $\Gamma_{Z_c(4700)} = 370_{-70-132}^{+70+70}$ MeV, can be safely absorbed into the pole residues $\lambda_{X/Z}$ [37]. Thus we take the zero width approximation, and expect that the predicted masses are reasonable.

On the other hand, the two-point correlation functions $\Pi_{\mu\nu}^{t,a/b}(p)$ can be calculated at the quark-gluon level via the operator product expansion method. We contract the u , d and c quark fields in the correlation functions $\Pi_{\mu\nu}^{t,a/b}(p)$ with the wick theorem and obtain the results:

$$\begin{aligned} \Pi_{\mu\nu}^{t,a}(p) &= i \frac{\epsilon^{ijk}\epsilon^{imn}\epsilon^{i'j'k'}\epsilon^{i'm'n'}}{2} \int d^4x e^{ip\cdot x} \\ &\left\{ \text{Tr} \left[C^{kk'}(x) C U^{jj'T}(x) C \right] \text{Tr} \left[C^{m'n}(-x) \gamma_\mu C D^{m'mT}(-x) C \gamma_\nu \right] \right. \\ &+ \text{Tr} \left[C^{kk'}(x) \gamma_\nu C U^{jj'T}(x) C \gamma_\mu \right] \text{Tr} \left[C^{m'n}(-x) C D^{m'mT}(-x) C \right] \\ &- t \text{Tr} \left[C^{kk'}(x) C U^{jj'T}(x) C \gamma_\mu \right] \text{Tr} \left[C^{m'n}(-x) C D^{m'mT}(-x) C \gamma_\nu \right] \\ &\left. - t \text{Tr} \left[C^{kk'}(x) \gamma_\nu C U^{jj'T}(x) C \right] \text{Tr} \left[C^{m'n}(-x) \gamma_\mu C D^{m'mT}(-x) C \right] \right\}, \quad (13) \end{aligned}$$

$$\begin{aligned} \Pi_{\mu\nu}^{t,b}(p) &= -i \frac{\epsilon^{ijk}\epsilon^{imn}\epsilon^{i'j'k'}\epsilon^{i'm'n'}}{2} \int d^4x e^{ip\cdot x} \\ &\left\{ \text{Tr} \left[C^{kk'}(x) \gamma_5 C U^{jj'T}(x) C \gamma_5 \right] \text{Tr} \left[C^{m'n}(-x) \gamma_\mu C D^{m'mT}(-x) C \gamma_\nu \right] \right. \\ &+ \text{Tr} \left[C^{kk'}(x) \gamma_\nu C U^{jj'T}(x) C \gamma_\mu \right] \text{Tr} \left[C^{m'n}(-x) \gamma_5 C D^{m'mT}(-x) C \gamma_5 \right] \\ &- t \text{Tr} \left[C^{kk'}(x) \gamma_5 C U^{jj'T}(x) C \gamma_\mu \right] \text{Tr} \left[C^{m'n}(-x) \gamma_5 C D^{m'mT}(-x) C \gamma_\nu \right] \\ &\left. - t \text{Tr} \left[C^{kk'}(x) \gamma_\nu C U^{jj'T}(x) C \gamma_5 \right] \text{Tr} \left[C^{m'n}(-x) \gamma_\mu C D^{m'mT}(-x) C \gamma_5 \right] \right\}, \quad (14) \end{aligned}$$

where the $U_{ij}(x)$, $D_{ij}(x)$ and $C_{ij}(x)$ are the full u , d and c quark propagators, respectively,

$$\begin{aligned} P_{ij}(x) &= \frac{i\delta_{ij}\not{x}}{2\pi^2x^4} - \frac{\delta_{ij}\langle\bar{q}q\rangle}{12} - \frac{\delta_{ij}x^2\langle\bar{q}g_s\sigma Gq\rangle}{192} - \frac{\delta_{ij}x^2\not{x}g_s^2\langle\bar{q}q\rangle^2}{7776} - \frac{ig_sG_{\alpha\beta}^n t_{ij}^n (\not{x}\sigma^{\alpha\beta} + \sigma^{\alpha\beta}\not{x})}{32\pi^2x^2} \\ &- \frac{\delta_{ij}x^4\langle\bar{q}q\rangle\langle GG\rangle}{27648} - \frac{1}{8}\langle\bar{q}_j\sigma^{\alpha\beta}q_i\rangle\sigma_{\alpha\beta} - \frac{1}{4}\langle\bar{q}_j\gamma_\mu q_i\rangle\gamma^\mu + \dots, \quad (15) \end{aligned}$$

$$\begin{aligned} C_{ij}(x) &= \frac{i}{(2\pi)^4} \int d^4k e^{-ik\cdot x} \left\{ \frac{\not{k} + m_c}{k^2 - m_c^2} \delta_{ij} - g_s t_{ij}^n G_{\alpha\beta}^n \frac{(\not{k} + m_c)\sigma^{\alpha\beta} + \sigma^{\alpha\beta}(\not{k} + m_c)}{4(k^2 - m_c^2)^2} \right. \\ &+ \frac{g_s t_{ij}^n D_\alpha G_{\beta\lambda}^n (f^{\lambda\alpha\beta} + f^{\lambda\beta\alpha})}{3(k^2 - m_c^2)^4} \\ &\left. - \frac{g_s^2 (t^n t^m)_{ij} G_{\alpha\beta}^n G_{\mu\nu}^m (f^{\alpha\beta\mu\nu} + f^{\alpha\mu\beta\nu} + f^{\alpha\nu\mu\beta})}{4(k^2 - m_c^2)^5} + \dots \right\}, \quad (16) \end{aligned}$$

$$\begin{aligned} f^{\lambda\alpha\beta} &= (\not{k} + m_c)\gamma^\lambda(\not{k} + m_c)\gamma^\alpha(\not{k} + m_c)\gamma^\beta(\not{k} + m_c), \\ f^{\alpha\beta\mu\nu} &= (\not{k} + m_c)\gamma^\alpha(\not{k} + m_c)\gamma^\beta(\not{k} + m_c)\gamma^\mu(\not{k} + m_c)\gamma^\nu(\not{k} + m_c), \quad (17) \end{aligned}$$

the $P_{ij}(x)$ denotes the light quark propagator $U_{ij}(x)$ or $D_{ij}(x)$, $t^n = \frac{\lambda^n}{2}$, the λ^n is the Gell-Mann matrix, and $D_\alpha = \partial_\alpha - ig_s G_\alpha^n t^n$ [38]. Then we compute the integrals both in the coordinate and momentum spaces, and obtain the correlation functions $\Pi_{\mu\nu}^{t,a/b}(p)$. In calculations, we carry out the operator product expansion to the vacuum condensates up to dimension-10. The vacuum condensates are the vacuum expectations of the operators \mathcal{O}_n , we take the truncations $n \leq 10$ and $k \leq 1$ for the operators in a consistent way, and discard the operators of the orders $\mathcal{O}(\alpha_s^k)$ with $k > 1$. In Eq.(15), we retain the terms $\langle \bar{q}_j \sigma_{\mu\nu} q_i \rangle$ and $\langle \bar{q}_j \gamma_\mu q_i \rangle$ originating from the Fierz re-arrangement of the $\langle q_i \bar{q}_j \rangle$ to absorb the gluons emitted from the heavy quark lines so as to extract the mixed condensates and four-quark condensates $\langle \bar{q} g_s \sigma G q \rangle$ and $g_s^2 \langle \bar{q} q \rangle^2$, respectively. One can consult Ref.[36] for some technical details in the operator product expansion. Once the analytical expressions of the correlation functions $\Pi_{\mu\nu}^{t,a/b}(p)$ are gotten, we can obtain the corresponding correlation functions $\Pi_0^{t,a/b}(p)$ of the scalar and pseudoscalar tetraquark states with: $\Pi_0^{t,a/b}(p) = \frac{p^\mu \Pi_{\mu\nu}^{t,a/b}(p)}{p^2 p_\nu}$. The QCD spectral densities $\rho^{Z_0^{t,a/b}}(s)$ of the scalar and pseudoscalar tetraquark states are obtained successfully through dispersion relation.

After getting the explicit expressions of the QCD spectral densities $\rho^{Z_0^{t,a/b}}(s)$, we take the quark-hadron duality below the continuum threshold value s_0 and perform Borel transform with respect to the variable $P^2 = -p^2$ to obtain the following QCD sum rules:

$$\lambda_{Z_0^{t,a/b}}^2 \exp\left(-\frac{M_{Z_0^{t,a/b}}^2}{T^2}\right) = \int_{4m_c^2}^{s_0} ds \rho^{Z_0^{t,a/b}}(s) \exp\left(-\frac{s}{T^2}\right), \quad (18)$$

where

$$\begin{aligned} \rho^{Z_0^{t,a/b}}(s) = & \rho_0^{t,a/b}(s) + \rho_3^{t,a/b}(s) + \rho_4^{t,a/b}(s) + \rho_5^{t,a/b}(s) + \rho_6^{t,a/b}(s) + \rho_7^{t,a/b}(s) \\ & + \rho_8^{t,a/b}(s) + \rho_{10}^{t,a/b}(s), \end{aligned} \quad (19)$$

the subscripts 0, 3, 4, 5, 6, 7, 8 and 10 denote the dimensions of the vacuum condensates in the operator product expansion, the T^2 denotes the Borel parameter. We collect the spectral densities $\rho^{Z_0^{t,a/b}}(s)$ explicitly in the appendix.

Differentiate Eq.(18) with respect to $\frac{1}{T^2}$ and eliminate the pole residues $\lambda_{Z_0^{t,a/b}}$, we obtain the QCD sum rules for the masses of the scalar and pseudoscalar tetraquark states,

$$M_{Z_0^{t,a/b}}^2 = \frac{\int_{4m_c^2}^{s_0} ds \frac{d}{d(-1/T^2)} \rho^{Z_0^{t,a/b}}(s) \exp\left(-\frac{s}{T^2}\right)}{\int_{4m_c^2}^{s_0} ds \rho^{Z_0^{t,a/b}}(s) \exp\left(-\frac{s}{T^2}\right)}. \quad (20)$$

3 Numerical results and discussions

In this section, we perform the numerical analysis. For the hadron mass, it is independent of the energy scale because of its observability. However, in our calculations, we discard the perturbative corrections and the operators of the orders $\mathcal{O}(\alpha_s^k)$ with $k > 1$ or the dimensions $n > 10$, and factorize the higher dimension operators into non-factorizable low dimension operators with the same quantum numbers of the vacuum. In addition, the variation of the heavy mass m_c depending on the energy scale leads to change of integral range $4m_c^2 - s_0$ of the variable ds . So we have to consider the energy scale dependence of the QCD sum rules. The input parameters at the QCD side are taken to be the standard condensate values $\langle \bar{q} q \rangle = -(0.24 \pm 0.01 \text{ GeV})^3$, $\langle \bar{q} g_s \sigma G q \rangle = m_0^2 \langle \bar{q} q \rangle$, $m_0^2 = (0.8 \pm 0.1) \text{ GeV}^2$, $\langle \frac{\alpha_s G G}{\pi} \rangle = (0.33 \text{ GeV})^4$ at the energy scale $\mu = 1 \text{ GeV}$ from the Gell-Mann-Oakes-Renner relation [38, 39, 40], and the \overline{MS} mass $m_c(m_c) = (1.275 \pm 0.025) \text{ GeV}$ from the Particle Data Group [2]. Moreover, we neglect the light quark masses and take into account the

energy-scale dependence of the quark condensate, mixed quark condensate and \overline{MS} mass from the renormalization group equation,

$$\begin{aligned}
\langle \bar{q}q \rangle(\mu) &= \langle \bar{q}q \rangle(Q) \left[\frac{\alpha_s(Q)}{\alpha_s(\mu)} \right]^{\frac{4}{9}}, \\
\langle \bar{q}g_s \sigma Gq \rangle(\mu) &= \langle \bar{q}g_s \sigma Gq \rangle(Q) \left[\frac{\alpha_s(Q)}{\alpha_s(\mu)} \right]^{\frac{2}{27}}, \\
m_c(\mu) &= m_c(m_c) \left[\frac{\alpha_s(\mu)}{\alpha_s(m_c)} \right]^{\frac{12}{25}}, \\
\alpha_s(\mu) &= \frac{1}{b_0 t'} \left[1 - \frac{b_1 \log t'}{b_0^2 t'} + \frac{b_1^2 (\log^2 t' - \log t' - 1) + b_0 b_2}{b_0^4 t'^2} \right], \tag{21}
\end{aligned}$$

where $t' = \log \frac{\mu^2}{\Lambda^2}$, $b_0 = \frac{33-2n_f}{12\pi}$, $b_1 = \frac{153-19n_f}{24\pi^2}$, $b_2 = \frac{2857-\frac{5033}{9}n_f+\frac{325}{27}n_f^2}{128\pi^3}$, $\Lambda = 213$ MeV, 296 MeV and 339 MeV for the flavors $n_f = 5, 4$ and 3 , respectively [2].

In Eq.(20), there are two free parameters: the Borel Parameter T^2 and the continuum threshold value s_0 . The extracted hadron mass is a function of the Borel parameter T^2 and the continuum threshold value s_0 . To obtain a reliable mass sum rule analysis, we impose two criteria on the hidden-charm tetraquark states to choose suitable working ranges for these two free parameters. The first criterion is the pole dominance on the phenomenological side, which require the pole contributions to be about (40 – 60)%. The pole contribution (PC) is defined as,

$$\text{PC} = \frac{\int_{4m_c^2}^{s_0} ds \rho^{Z_0^{t,a/b}}(s) \exp\left(-\frac{s}{T^2}\right)}{\int_{4m_c^2}^{\infty} ds \rho^{Z_0^{t,a/b}}(s) \exp\left(-\frac{s}{T^2}\right)}. \tag{22}$$

The second criterion is the convergence of the operator product expansion. To judge the convergence, we calculate the contributions D_i in the operator product expansion with the formula,

$$D_i = \frac{\int_{4m_c^2}^{s_0} ds \rho_i^{Z_0^{t,a/b}}(s) \exp\left(-\frac{s}{T^2}\right)}{\int_{4m_c^2}^{s_0} ds \rho^{Z_0^{t,a/b}}(s) \exp\left(-\frac{s}{T^2}\right)}, \tag{23}$$

where the index i denotes the dimension of the vacuum condensates.

To search for the continuum threshold value s_0 more precisely, we take into account the mass gaps between the ground states and the first radial excited states, which are usually taken as (0.4 – 0.6) GeV in the tetraquark sector. For examples, the $Z(4430)$ is tentatively assigned to be the first radial excitation of the $Z_c(3900)$ according to the analogous decays, $Z_c(3900)^\pm \rightarrow J/\psi \pi^\pm$, $Z(4430)^\pm \rightarrow \psi' \pi^\pm$ and the mass differences $M_{Z(4430)} - M_{Z_c(3900)} = 576$ MeV, $M_{\psi'} - M_{J/\psi} = 589$ MeV [41-44]; the $X(3915)$ and $X(4500)$ are assigned to be the ground state and the first radial excited state of the axialvector-diquark-axialvector-antidiquark type scalar $c\bar{s}c\bar{s}$ tetraquark states, respectively, and their mass difference is $M_{X(4500)} - M_{X(3915)} = 588$ MeV [45]. The relation

$$\sqrt{s_0} = M_{X/Y/Z} + (0.4 - 0.6) \text{ GeV}, \tag{24}$$

serves as a constraint on the masses of the hidden-charm tetraquark states.

In this article, we take the energy scale μ as a free parameter and evolve all the input parameters in the QCD spectral density to the special energy scale determined by the empirical formula,

$$\mu = \sqrt{M_{X/Y/Z}^2 - (2\mathbb{M}_c)^2}, \tag{25}$$

with the effective c -quark mass $\mathbb{M}_c = 1.82$ GeV. The heavy tetraquark system could be described by a double-well potential with two light quarks $q'\bar{q}$ lying in the two wells respectively. In the heavy

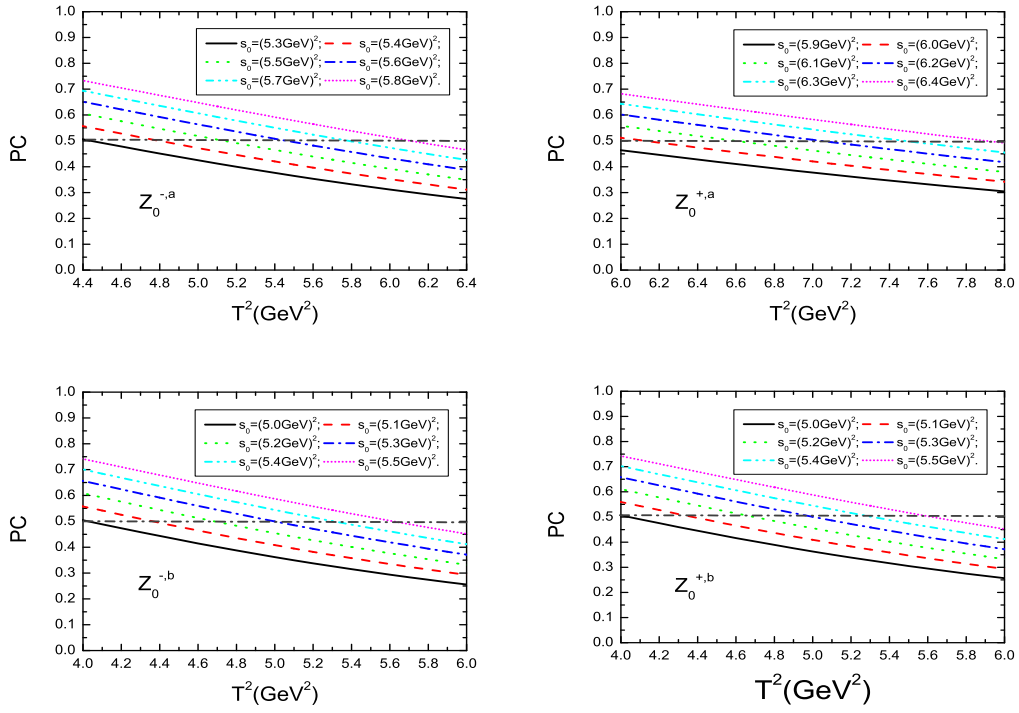


Figure 1: The pole contributions with variations of the Borel parameters T^2 and threshold parameters s_0 .

quark limit, the c quark can be taken as a static well potential, which binds the light quark q' to form a diquark in the color antitriplet channel or binds the light antiquark \bar{q} to form a meson in the color singlet channel (or a meson-like state in the color octet channel). Then the heavy tetraquark states are characterized by the effective heavy quark masses M_c (or constituent quark masses) and the virtuality $V = \sqrt{M_{X/Y/Z}^2 - (2M_c)^2}$. It is natural to take the energy scale $\mu = V$. For a better understanding of the energy scale dependence in Eq.(25), one can refer to Refs.[35,36,46-49], where the authors study the energy scale dependence of the QCD sum rules for the hidden-charm tetraquark states and molecular states in detail, and suggest the above energy scale formula for the first time. The energy scale formula works well for the $X(3872)$, $Z_c(3885/3900)$, $X^*(3860)$, $Y(3915)$, $Z_c(4020/4025)$, $Z(4430)$, $X(4500)$, $Y(4630/4660)$, $X(4700)$ in the scenario of tetraquark states. Actually, the formula put another constraint on the masses of the hidden-charm tetraquark states. In our calculations, we observe that the values of the masses M_Z decrease slightly with increase of the energy scales μ from QCD sum rules in Eq.(20), while Eq.(25) indicates that the value of the masses M_Z increase when the energy scales μ increase. Thus there exist optimal energy scales, which lead to reasonable masses M_Z .

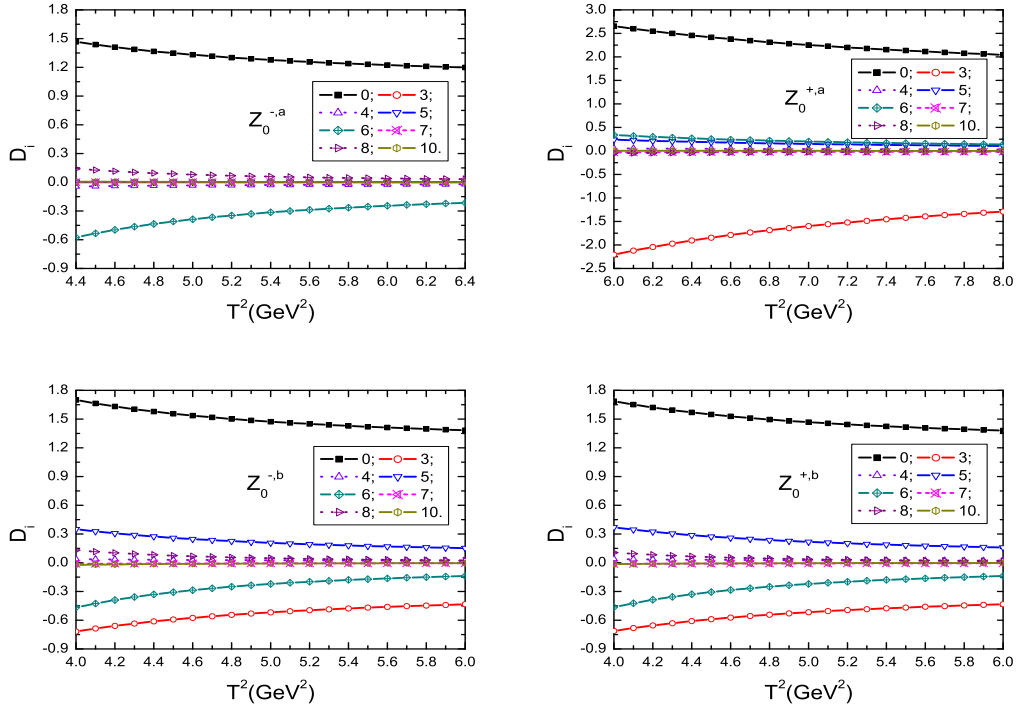


Figure 2: The contributions of different terms in the operator product expansion with variations of the Borel parameters T^2 , where the 0, 3, 4, 5, 6, 7, 8, 10 denote the dimensions of the vacuum condensates.

In Fig.1, we show the variations of the pole contributions with respect to the Borel parameters T^2 for different values of the continuum thresholds s_0 at the energy scales $\mu = 3.6$ GeV, 4.4 GeV, 3.2 GeV and 3.2 GeV for the tetraquark states $Z_0^{-,a}$, $Z_0^{+,a}$, $Z_0^{-,b}$ and $Z_0^{+,b}$, respectively. In Fig.2, the contributions of different terms in the operator product expansion are plotted with variations of the Borel parameters T^2 at the parameters $s_0 = 5.6$ GeV, $\mu = 3.6$ GeV; $s_0 = 6.2$ GeV, $\mu = 4.4$ GeV; $s_0 = 5.3$ GeV, $\mu = 3.2$ GeV and $s_0 = 5.3$ GeV, $\mu = 3.2$ GeV for the tetraquark states $Z_0^{-,a}$, $Z_0^{+,a}$, $Z_0^{-,b}$ and $Z_0^{+,b}$, respectively. From the figures, we can choose the optimal Borel parameters and

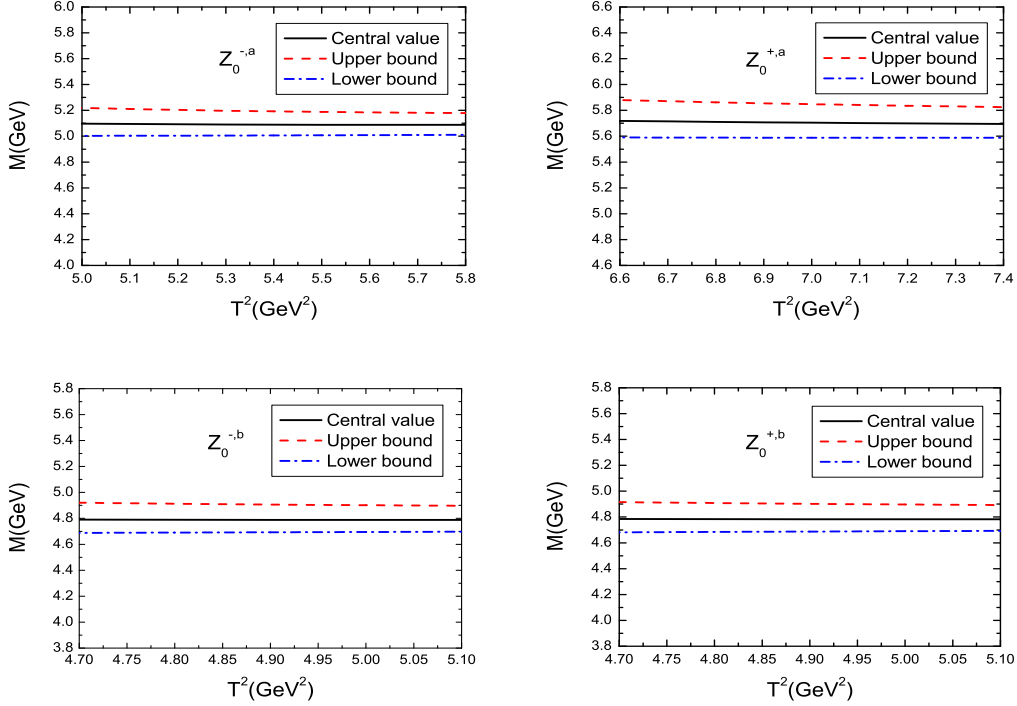


Figure 3: The masses with variations of the Borel parameters T^2 .

threshold parameters to satisfy the two criteria of the QCD sum rules. To explain the procedure, we take the scalar tetraquark state $Z_0^{-,a}$ with $J^{PC} = 0^{++}$ as an example. From the first panel of Fig.1, we can see that the values $\sqrt{s_0} \leq 5.4$ GeV are too small to satisfy the pole dominance condition and result in reasonable Borel windows. In the first panel of Fig.2, the contributions of different terms change quickly with respect to the Borel parameter at the region $T^2 < 5.0$ GeV², which does not warrant platform for the mass. At the value $T^2 = 5.0$ GeV², the $D_0, D_3, D_4, D_5, D_6, D_7, D_8, D_{10}$ are 1.331, 0.000, -0.034, 0.003, -0.386, 0.002, 0.080, 0.004 respectively for the tetraquark state $Z_0^{-,a}$ and the total contributions are normalized to be 1. Accordingly, the $T^2 \geq 5.0$ GeV² is taken tentatively, the perturbative term plays an important role, and the convergent behavior in the operator product expansion is very good. If we take the values $\sqrt{s_0} = (5.5 - 5.7)$ GeV and $T^2 = (5.0 - 5.8)$ GeV², the pole contribution is about (42 - 61)% for the state $Z_0^{-,a}$. The pole dominance condition is well satisfied. Similarly, we obtain the Borel parameters, continuum thresholds and the pole contributions for all tetraquark states $Z_0^{\pm,a/b}$, which are shown explicitly in Table 1.

	μ (GeV)	T^2 (GeV ²)	$\sqrt{s_0}$ (GeV)	pole	M_Z (GeV)	λ_Z (GeV ⁴)
$Z_0^{-,a} (0^{++})$	3.6	5.0 - 5.8	5.6 ± 0.1	(42 - 61) %	$5.09_{-0.08}^{+0.13}$	$(1.58_{-0.16}^{+0.20}) \times 10^{-2}$
$Z_0^{+,a} (0^{+-})$	4.4	6.6 - 7.4	6.2 ± 0.1	(43 - 58) %	$5.70_{-0.12}^{+0.18}$	$(4.08_{-0.35}^{+0.42}) \times 10^{-2}$
$Z_0^{-,b} (0^{-+})$	3.2	4.7 - 5.1	5.3 ± 0.1	(44 - 59) %	$4.79_{-0.09}^{+0.13}$	$(1.45_{-0.15}^{+0.17}) \times 10^{-2}$
$Z_0^{+,b} (0^{--})$	3.2	4.7 - 5.1	5.3 ± 0.1	(44 - 59) %	$4.78_{-0.09}^{+0.13}$	$(1.44_{-0.15}^{+0.17}) \times 10^{-2}$

Table 1: The energy scales, Borel parameters, continuum threshold parameters, pole contributions, masses and pole residues for the scalar and pseudoscalar tetraquark states.

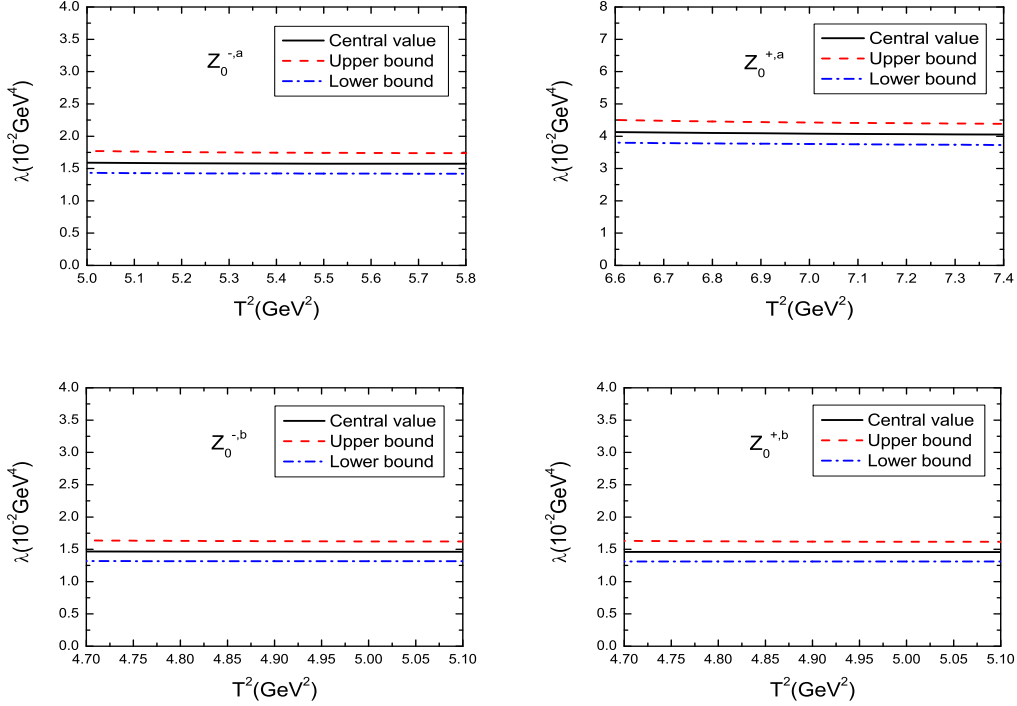


Figure 4: The pole residues with variations of the Borel parameters T^2 .

We take into account all uncertainties of the input parameters, and obtain the values of the masses and pole residues of the tetraquark states, which are shown in Table 1 and Figs.3-4. From Figs.3-4, we can see that the Borel platforms exist. On the other hand, from Table 1, we can see that the energy scale formula $\mu = \sqrt{M_{X/Y/Z}^2 - (2M_c)^2}$ and the relation $\sqrt{s_0} = M_{X/Y/Z} + (0.4-0.6)$ GeV are well satisfied. The numerical results indicate that none of the tetraquark states $Z_0^{\pm, a/b}$ is the lowest hidden charmed tetraquark state, whose mass is about 3.82 GeV [50]; the charge conjugation partners have almost degenerate masses for the pseudoscalar tetraquark states $Z_0^{\pm, b}$, while there is a considerably large energy gap about 610 MeV between the masses of the $C = +$ and $C = -1$ scalar tetraquark states $Z_0^{\pm, a}$; the mass predictions of the scalar tetraquark states are larger than the counterparts of the pseudoscalar tetraquark states because the scalar tetraquark states have the $C \otimes C$ type substructure and the pseudoscalar tetraquark states have more stable $C\gamma_5 \otimes C$ type and $C \otimes \gamma_5 C$ type substructures, which can be found in Eqs.(5)-(6). A meson may have a lot of Fock states with different constituents, such as $\bar{q}q$, $\bar{q}qg$, $\bar{q}q\bar{q}q$, etc. These mesons we study in this article have non-vanishing couplings with the tetraquark currents, thus these mesons contain the tetraquark constituent. The present predictions can be confronted with the experimental data in the future at the BESIII, LHCb and Belle-II.

Using the masses obtained above, we study the possible hadronic decay patterns of the scalar and pseudoscalar hidden-charm tetraquark states $Z_0^{\pm, a/b}$. It's known that a hidden-charm tetraquark state composed of a diquark and antidiquark pair can decay easily into a pair of open-charm D mesons or one charmonium state plus a light meson through quark rearrangement. Such two-body strong decays are Okubo-Zweig-Iizuka super-allowed. Considering the conservation of the angular momentum, parity, charge conjugation and isospin, we list out the possible strong decays of the

$$\begin{aligned}
& Z_0^{\pm, a/b}, \\
Z_0^{-, a} (0^{++}) & \longrightarrow \eta_c \pi^+, J/\psi \rho^+(770), \psi(3770) \rho^+(770), \chi_{c0} a_0^+(980), \chi_{c1} a_1^+(1260), h_c b_1^+(1235), \\
& \bar{D}^0 D^+, \bar{D}^{*0}(2007) D^{*+}(2010), \bar{D}_0^{*0}(2400) D_0^{*+}(2400), \bar{D}_1^0(2420) D_1^+(2420), \\
& \bar{D}_1^0(2430) D_1^+(2430), \\
Z_0^{+, a} (0^{+-}) & \longrightarrow J/\psi \pi_1^+(1400), \psi(3770) \pi_1^+(1400), \chi_{c1} b_1^+(1235), h_c a_1^+(1260), \bar{D}^0 D^+, \\
& \bar{D}^{*0}(2007) D^{*+}(2010), \bar{D}_0^{*0}(2400) D_0^{*+}(2400), \bar{D}_1^0(2420) D_1^+(2420), \\
& \bar{D}_1^0(2430) D_1^+(2430), \\
Z_0^{-, b} (0^{-+}) & \longrightarrow \eta_c a_0^+(980), J/\psi b_1^+(1235), \chi_{c0} \pi^+, h_c \rho^+(770), \bar{D}_0^{*0}(2400) D^+, \bar{D}^0 D_0^{*+}(2400), \\
& \bar{D}_1^0(2420) D^{*+}(2010), \bar{D}_1^0(2430) D^{*+}(2010), \\
Z_0^{+, b} (0^{--}) & \longrightarrow J/\psi a_1^+(1260), \chi_{c1} \rho^+(770), \bar{D}_0^{*0}(2400) D^+, \bar{D}^0 D_0^{*+}(2400), \\
& \bar{D}_1^0(2420) D^{*+}(2010), \bar{D}_1^0(2430) D^{*+}(2010). \tag{26}
\end{aligned}$$

Under the restriction of charge conjugation, the decay modes of double open-charm D mesons are dominant for the scalar and pseudoscalar tetraquark states with negative charge conjugation. For the scalar tetraquark states, the $Z_0^{-, a}$ is much narrower than the $Z_0^{+, a}$, as the mass of the $Z_0^{-, a}$ is much smaller. Thus, compared to the $Z_0^{+, a}$, the $Z_0^{-, a}$ will be prime candidate for observation.

4 Conclusion

In this article, based on the diquark configuration, we use the scalar, pseudoscalar, axialvector diquarks and their corresponding antidiquarks to construct the vector and axial-vector interpolating tetraquark currents, which can couple to the scalar and pseudoscalar tetraquark states respectively. Then we distinguish the charge conjugations of the interpolating currents. In calculations, we consider the contributions of the vacuum condensates up to dimension 10, use the empirical energy scale formula to determine the ideal energy scales of the QCD spectral densities, and study the ground state masses and pole residues of the hidden-charm tetraquark states with quantum numbers $J^{PC} = 0^{+\pm}$ and $0^{-\pm}$. The numerical results of the masses $M_{Z_0^{\pm, a/b}}$ show that the charge conjugation partners have almost degenerate masses for the pseudoscalar tetraquark states, while there is a considerably large energy gap about 610 MeV between the masses of the $C = +$ and $C = -1$ scalar tetraquark states, which is especially interesting. And the mass predictions of the scalar tetraquark states are larger than the counterparts of the pseudoscalar tetraquark states. Moreover, we briefly discuss the possible decay patterns of the tetraquark states. Our studies on the tetraquark states can be useful for their searches in future experiments at facilities such as BESIII, BelleII, LHCb, etc.

Acknowledgements

This work is supported by National Natural Science Foundation, Grant Number 11775079.

Appendix

The explicit expressions of the QCD spectral densities $\rho^{Z_0^{t,a/b}}(s)$ for the scalar and pseudoscalar tetraquark states,

$$\begin{aligned} \rho_0^{t,a}(s) &= \frac{1}{1024\pi^6 s} \int_{y_i}^{y_f} dy \int_{z_i}^{1-y} dz yz(1-y-z)^3 (s - \hat{m}_c^2)^2 (7s^2 - 2\hat{m}_c^2 s - \hat{m}_c^4) \\ &\quad + \frac{tm_c^2}{1536\pi^6 s} \int_{y_i}^{y_f} dy \int_{z_i}^{1-y} dz (1-y-z)^3 (s - \hat{m}_c^2)^2 (7s - \hat{m}_c^2) , \end{aligned} \quad (27)$$

$$\rho_0^{t,b}(s) = \frac{1}{1024\pi^6 s} \int_{y_i}^{y_f} dy \int_{z_i}^{1-y} dz yz(1-y-z)^3 (s - \hat{m}_c^2)^2 (7s^2 - 2\hat{m}_c^2 s - \hat{m}_c^4) , \quad (28)$$

$$\rho_3^{t,a}(s) = \frac{(1+t)m_c \langle \bar{q}q \rangle}{64\pi^4 s} \int_{y_i}^{y_f} dy \int_{z_i}^{1-y} dz (y+z)(1-y-z)(s - \hat{m}_c^2)(5s - \hat{m}_c^2) , \quad (29)$$

$$\rho_3^{t,b}(s) = \frac{3m_c \langle \bar{q}q \rangle}{64\pi^4 s} \int_{y_i}^{y_f} dy \int_{z_i}^{1-y} dz (y+z)(1-y-z)(s - \hat{m}_c^2)^2 , \quad (30)$$

$$\begin{aligned} \rho_4^{t,a}(s) &= -\frac{m_c^2}{768\pi^4 s} \langle \frac{\alpha_s GG}{\pi} \rangle \int_{y_i}^{y_f} dy \int_{z_i}^{1-y} dz \left(\frac{z}{y^2} + \frac{y}{z^2} \right) (1-y-z)^3 \left[\hat{m}_c^2 + \frac{s^2}{3} \delta(s - \hat{m}_c^2) \right] \\ &\quad - \frac{tm_c^4}{4608\pi^4 s} \langle \frac{\alpha_s GG}{\pi} \rangle \int_{y_i}^{y_f} dy \int_{z_i}^{1-y} dz \left(\frac{1}{y^3} + \frac{1}{z^3} \right) (1-y-z)^3 [1 + 2s\delta(s - \hat{m}_c^2)] \\ &\quad + \frac{1}{512\pi^4} \langle \frac{\alpha_s GG}{\pi} \rangle \int_{y_i}^{y_f} dy \int_{z_i}^{1-y} dz (y+z)(1-y-z)^2 (5s - 4\hat{m}_c^2) \\ &\quad - \frac{tm_c^2}{2304\pi^4 s} \langle \frac{\alpha_s GG}{\pi} \rangle \int_{y_i}^{y_f} dy \int_{z_i}^{1-y} dz \frac{(1-y-z)^2}{yz} (s - \hat{m}_c^2) \\ &\quad + \frac{tm_c^2}{13824\pi^4 s} \langle \frac{\alpha_s GG}{\pi} \rangle \int_{y_i}^{y_f} dy \int_{z_i}^{1-y} dz \left\{ \left[\frac{1}{yz} + 9 \left(\frac{1}{y^2} + \frac{1}{z^2} \right) \right] (1-y-z) \right. \\ &\quad \left. + \frac{27}{2} \left(\frac{1}{y} + \frac{1}{z} \right) \right\} (1-y-z)^2 (3s - \hat{m}_c^2) , \end{aligned} \quad (31)$$

$$\begin{aligned} \rho_4^{t,b}(s) &= -\frac{m_c^2}{768\pi^4 s} \langle \frac{\alpha_s GG}{\pi} \rangle \int_{y_i}^{y_f} dy \int_{z_i}^{1-y} dz \left(\frac{y}{z^2} + \frac{z}{y^2} \right) (1-y-z)^3 \left[\hat{m}_c^2 + \frac{s^2}{3} \delta(s - \hat{m}_c^2) \right] \\ &\quad + \frac{1}{512\pi^4} \langle \frac{\alpha_s GG}{\pi} \rangle \int_{y_i}^{y_f} dy \int_{z_i}^{1-y} dz (y+z)(1-y-z)^2 (5s - 4\hat{m}_c^2) \\ &\quad + \frac{tm_c^2}{2304\pi^4 s} \langle \frac{\alpha_s GG}{\pi} \rangle \int_{y_i}^{y_f} dy \int_{z_i}^{1-y} dz \\ &\quad \left[\frac{(1-y-z)^2}{yz} + 2 - 2 \left(\frac{1}{y} + \frac{1}{z} \right) (1-y-z) \right] (s - \hat{m}_c^2) \\ &\quad - \frac{tm_c^2}{13824\pi^4 s} \langle \frac{\alpha_s GG}{\pi} \rangle \int_{y_i}^{y_f} dy \int_{z_i}^{1-y} dz \\ &\quad \left[\frac{(1-y-z)^3}{yz} + 6(1-y-z) - 3 \left(\frac{1}{y} + \frac{1}{z} \right) (1-y-z)^2 \right] (3s - \hat{m}_c^2) , \end{aligned} \quad (32)$$

$$\begin{aligned}
\rho_5^{t,a}(s) &= \frac{m_c \langle \bar{q} g_s \sigma G q \rangle}{128\pi^4 s} \int_{y_i}^{y_f} dy \int_{z_i}^{1-y} dz \{t[1-2(y+z)] - (y+z)\} (3s - \hat{m}_c^2) \\
&+ \frac{m_c \langle \bar{q} g_s \sigma G q \rangle}{128\pi^4 s} \int_{y_i}^{y_f} dy \int_{z_i}^{1-y} dz \left(\frac{y}{z} + \frac{z}{y} \right) (1-y-z) \hat{m}_c^2 \\
&- \frac{t m_c \langle \bar{q} g_s \sigma G q \rangle}{384\pi^4 s} \int_{y_i}^{y_f} dy \int_{z_i}^{1-y} dz \left(\frac{y}{z} + \frac{z}{y} \right) (1-y-z) (s - \hat{m}_c^2) , \quad (33)
\end{aligned}$$

$$\begin{aligned}
\rho_5^{t,b}(s) &= + \frac{m_c \langle \bar{q} g_s \sigma G q \rangle}{384\pi^4 s} \int_{y_i}^{y_f} dy \int_{z_i}^{1-y} dz \left[t \left(\frac{y}{z} + \frac{z}{y} \right) (1-y-z) - (t+9)(y+z) \right] (s - \hat{m}_c^2) \\
&- \frac{m_c \langle \bar{q} g_s \sigma G q \rangle}{128\pi^4 s} \int_{y_i}^{y_f} dy \int_{z_i}^{1-y} dz \left(\frac{y}{z} + \frac{z}{y} \right) (1-y-z) \hat{m}_c^2 , \quad (34)
\end{aligned}$$

$$\begin{aligned}
\rho_6^{t,a}(s) &= \frac{m_c^2 \langle \bar{q} q \rangle^2}{12\pi^2 s} \int_{y_i}^{y_f} dy + \frac{t \langle \bar{q} q \rangle^2}{24\pi^2 s} \int_{y_i}^{y_f} dy y (1-y) (3s - \tilde{m}_c^2) \\
&+ \frac{t m_c^2 g_s^2 \langle \bar{q} q \rangle^2}{5184\pi^4 s} \int_{y_i}^{y_f} dy \int_{z_i}^{1-y} dz \left[4 - 5 \left(\frac{1}{y} + \frac{1}{z} \right) (1-y-z) \right] [1 + 2s\delta(s - \hat{m}_c^2)] \\
&- \frac{g_s^2 \langle \bar{q} q \rangle^2}{2592\pi^4 s} \int_{y_i}^{y_f} dy \int_{z_i}^{1-y} dz \left\{ \left[(y+z) + 14 \left(\frac{y}{z} + \frac{z}{y} \right) \right] (1-y-z) - 12yz \right\} \hat{m}_c^2 \\
&+ \frac{g_s^2 \langle \bar{q} q \rangle^2}{864\pi^4} \int_{y_i}^{y_f} dy \int_{z_i}^{1-y} dz \left[3 \left(\frac{y}{z} + \frac{z}{y} \right) - 4(y+z) \right] (1-y-z) \\
&- \frac{g_s^2 \langle \bar{q} q \rangle^2}{3888\pi^4} \int_{y_i}^{y_f} dy \int_{z_i}^{1-y} dz [5(y+z)(1-y-z) - 6yz] s\delta(s - \hat{m}_c^2) \\
&+ \frac{m_c^2 g_s^2 \langle \bar{q} q \rangle^2}{7776\pi^4 s} \int_{y_i}^{y_f} dy \int_{z_i}^{1-y} dz \left(\frac{y}{z^2} + \frac{z}{y^2} \right) (1-y-z) [23 - 5s\delta(s - \hat{m}_c^2)] , \quad (35)
\end{aligned}$$

$$\begin{aligned}
\rho_6^{t,b}(s) &= - \frac{m_c^2 \langle \bar{q} q \rangle^2}{12\pi^2 s} \int_{y_i}^{y_f} dy + \frac{g_s^2 \langle \bar{q} q \rangle^2}{864\pi^4} \int_{y_i}^{y_f} dy \int_{z_i}^{1-y} dz \left[3 \left(\frac{y}{z} + \frac{z}{y} \right) - 4(y+z) \right] (1-y-z) \\
&- \frac{g_s^2 \langle \bar{q} q \rangle^2}{2592\pi^4 s} \int_{y_i}^{y_f} dy \int_{z_i}^{1-y} dz \left\{ \left[(y+z) + 14 \left(\frac{y}{z} + \frac{z}{y} \right) \right] (1-y-z) - 12yz \right\} \hat{m}_c^2 \\
&- \frac{g_s^2 \langle \bar{q} q \rangle^2}{3888\pi^4} \int_{y_i}^{y_f} dy \int_{z_i}^{1-y} dz [5(y+z)(1-y-z) - 6yz] s\delta(s - \hat{m}_c^2) \\
&+ \frac{m_c^2 g_s^2 \langle \bar{q} q \rangle^2}{7776\pi^4 s} \int_{y_i}^{y_f} dy \int_{z_i}^{1-y} dz \left(\frac{y}{z^2} + \frac{z}{y^2} \right) (1-y-z) [23 - 5s\delta(s - \hat{m}_c^2)] , \quad (36)
\end{aligned}$$

$$\begin{aligned}
\rho_7^{t,a}(s) &= \frac{m_c \langle \bar{q} q \rangle}{192\pi^2 s} \langle \frac{\alpha_s GG}{\pi} \rangle \int_{y_i}^{y_f} dy \int_{z_i}^{1-y} dz \left[(1+t) \left(\frac{y}{z^2} + \frac{z}{y^2} \right) (1-y-z) + \frac{t}{2} \left(\frac{y}{z} + \frac{z}{y} \right) + 3 \right] \\
&+ \frac{m_c \langle \bar{q} q \rangle}{96\pi^2} \langle \frac{\alpha_s GG}{\pi} \rangle \int_{y_i}^{y_f} dy \int_{z_i}^{1-y} dz \left[(1+t) \left(\frac{y}{z^2} + \frac{z}{y^2} \right) (1-y-z) + \frac{t}{2} \left(\frac{y}{z} + \frac{z}{y} \right) + 1 \right] \\
&\delta(s - \hat{m}_c^2) - \frac{(1+t) m_c^3 \langle \bar{q} q \rangle}{576\pi^2} \langle \frac{\alpha_s GG}{\pi} \rangle \int_{y_i}^{y_f} dy \int_{z_i}^{1-y} dz \left(\frac{1}{y^2} + \frac{1}{z^2} + \frac{y}{z^3} + \frac{z}{y^3} \right) (1-y-z) \\
&\left(\frac{1}{s} + \frac{2}{T^2} \right) \delta(s - \hat{m}_c^2) + \frac{(1+t) m_c \langle \bar{q} q \rangle}{1152\pi^2 s} \langle \frac{\alpha_s GG}{\pi} \rangle \int_{y_i}^{y_f} dy [1 + 2s\delta(s - \tilde{m}_c^2)] , \quad (37)
\end{aligned}$$

$$\begin{aligned}
\rho_7^{t,b}(s) &= \frac{m_c \langle \bar{q}q \rangle}{576\pi^2 s} \langle \frac{\alpha_s GG}{\pi} \rangle \int_{y_i}^{y_f} dy \int_{z_i}^{1-y} dz \left\{ \left[9 \left(\frac{y}{z^2} + \frac{z}{y^2} \right) - t \left(\frac{1}{y} + \frac{1}{z} \right) \right] (1-y-z) + (2t+3) \right\} \\
&\quad - \frac{m_c^3 \langle \bar{q}q \rangle}{192\pi^2 s} \langle \frac{\alpha_s GG}{\pi} \rangle \int_{y_i}^{y_f} dy \int_{z_i}^{1-y} dz \left(\frac{1}{y^2} + \frac{1}{z^2} + \frac{y}{z^3} + \frac{z}{y^3} \right) (1-y-z) \delta(s - \hat{m}_c^2) \\
&\quad + \frac{m_c \langle \bar{q}q \rangle}{384\pi^2 s} \langle \frac{\alpha_s GG}{\pi} \rangle \int_{y_i}^{y_f} dy , \tag{38}
\end{aligned}$$

$$\begin{aligned}
\rho_8^{t,a}(s) &= -\frac{\langle \bar{q}q \rangle \langle \bar{q}g_s \sigma Gq \rangle}{24\pi^2} \int_{y_i}^{y_f} dy \left(\frac{2m_c^2}{s} + \frac{m_c^2}{T^2} - \frac{1}{4} \right) \delta(s - \tilde{m}_c^2) \\
&\quad - \frac{7t \langle \bar{q}q \rangle \langle \bar{q}g_s \sigma Gq \rangle}{48\pi^2} \int_{y_i}^{y_f} dy y(1-y) \left(1 + \frac{2s}{7T^2} \right) \delta(s - \tilde{m}_c^2) \\
&\quad + \frac{t \langle \bar{q}q \rangle \langle \bar{q}g_s \sigma Gq \rangle}{192\pi^2 s} \int_{y_i}^{y_f} dy [1 + 2s\delta(s - \tilde{m}_c^2) - 12y(1-y)] , \tag{39}
\end{aligned}$$

$$\begin{aligned}
\rho_8^{t,b}(s) &= \frac{\langle \bar{q}q \rangle \langle \bar{q}g_s \sigma Gq \rangle}{24\pi^2} \int_{y_i}^{y_f} dy \left[\frac{2m_c^2}{s} + \frac{m_c^2}{T^2} - \frac{1}{4} \right] \delta(s - \tilde{m}_c^2) \\
&\quad - \frac{t \langle \bar{q}q \rangle \langle \bar{q}g_s \sigma Gq \rangle}{288\pi^2 s} \int_{y_i}^{y_f} dy , \tag{40}
\end{aligned}$$

$$\begin{aligned}
\rho_{10}^{t,a}(s) &= t \left(\frac{\langle \bar{q}g_s \sigma Gq \rangle^2}{32\pi^2} + \frac{\langle \bar{q}q \rangle^2}{36} \langle \frac{\alpha_s GG}{\pi} \rangle \right) \int_{y_i}^{y_f} dy y(1-y) \left(\frac{1}{s} + \frac{3}{2T^2} + \frac{3s}{4T^4} + \frac{s^2}{6T^6} \right) \delta(s - \tilde{m}_c^2) \\
&\quad + \left(\frac{m_c^2 \langle \bar{q}g_s \sigma Gq \rangle^2}{32\pi^2 s^2} + \frac{m_c^2 \langle \bar{q}q \rangle^2}{36s^2} \langle \frac{\alpha_s GG}{\pi} \rangle \right) \int_{y_i}^{y_f} dy \left(1 + \frac{s}{T^2} + \frac{s^2}{2T^4} + \frac{s^3}{6T^6} \right) \delta(s - \tilde{m}_c^2) \\
&\quad - \frac{\langle \bar{q}g_s \sigma Gq \rangle^2}{192\pi^2 s} \int_{y_i}^{y_f} dy \left(1 + \frac{s}{T^2} + \frac{s^2}{2T^4} \right) \delta(s - \tilde{m}_c^2) \\
&\quad - \frac{t \langle \bar{q}g_s \sigma Gq \rangle^2}{384\pi^2 s} \int_{y_i}^{y_f} dy \left(1 + \frac{3s}{2T^2} + \frac{s^2}{T^4} \right) \delta(s - \tilde{m}_c^2) \\
&\quad + \frac{m_c^2 \langle \bar{q}q \rangle^2}{72s^2} \langle \frac{\alpha_s GG}{\pi} \rangle \int_{y_i}^{y_f} dy \left[\frac{1}{y^2} + \frac{1}{(1-y)^2} \right] \left(1 + \frac{s}{T^2} \right) \delta(s - \tilde{m}_c^2) \\
&\quad - \frac{m_c^4 \langle \bar{q}q \rangle^2}{108s^3} \langle \frac{\alpha_s GG}{\pi} \rangle \int_{y_i}^{y_f} dy \left[\frac{1}{y^3} + \frac{1}{(1-y)^3} \right] \left(1 + \frac{s}{T^2} + \frac{s^2}{2T^4} \right) \delta(s - \tilde{m}_c^2) \\
&\quad - \frac{tm_c^2 \langle \bar{q}q \rangle^2}{432s^2} \langle \frac{\alpha_s GG}{\pi} \rangle \int_{y_i}^{y_f} dy \left[\frac{y}{(1-y)^2} + \frac{1-y}{y^2} \right] \left(1 + \frac{s}{T^2} + \frac{2s^2}{T^4} \right) \delta(s - \tilde{m}_c^2) , \tag{41}
\end{aligned}$$

$$\begin{aligned}
\rho_{10}^{t,b}(s) = & - \left(\frac{m_c^2 \langle \bar{q} g_s \sigma G q \rangle^2}{32\pi^2 s^2} + \frac{m_c^2 \langle \bar{q} q \rangle^2 \langle \alpha_s G G \rangle}{36s^2 \pi} \right) \int_{y_i}^{y_f} dy \left(1 + \frac{s}{T^2} + \frac{s^2}{2T^4} + \frac{s^3}{6T^6} \right) \delta(s - \tilde{m}_c^2) \\
& - \frac{m_c^2 \langle \bar{q} q \rangle^2 \langle \alpha_s G G \rangle}{72s^2 \pi} \int_{y_i}^{y_f} dy \left[\frac{1}{y^2} + \frac{1}{(1-y)^2} \right] \left(1 + \frac{s}{T^2} \right) \delta(s - \tilde{m}_c^2) \\
& + \frac{m_c^4 \langle \bar{q} q \rangle^2 \langle \alpha_s G G \rangle}{108s^3 \pi} \int_{y_i}^{y_f} dy \left[\frac{1}{y^3} + \frac{1}{(1-y)^3} \right] \left(1 + \frac{s}{T^2} + \frac{s^2}{2T^4} \right) \delta(s - \tilde{m}_c^2) \\
& + \frac{t \langle \bar{q} q \rangle^2 \langle \alpha_s G G \rangle}{432s \pi} \int_{y_i}^{y_f} dy \delta(s - \tilde{m}_c^2) + \frac{t \langle \bar{q} g_s \sigma G q \rangle^2}{256\pi^2 s} \int_{y_i}^{y_f} dy \left(1 + \frac{2s}{9T^2} \right) \delta(s - \tilde{m}_c^2) \\
& + \frac{\langle \bar{q} g_s \sigma G q \rangle^2}{192\pi^2 s} \int_{y_i}^{y_f} dy \left(1 + \frac{s}{T^2} + \frac{s^2}{2T^4} \right) \delta(s - \tilde{m}_c^2), \tag{42}
\end{aligned}$$

where $y_f = \frac{1+\sqrt{1-4m_c^2/s}}{2}$, $y_i = \frac{1-\sqrt{1-4m_c^2/s}}{2}$, $z_i = \frac{ym_c^2}{ys-m_c^2}$, $\hat{m}_c^2 = \frac{(y+z)m_c^2}{yz}$, $\tilde{m}_c^2 = \frac{m_c^2}{y(1-y)}$, $\int_{y_i}^{y_f} dy \rightarrow \int_0^1$, $\int_{z_i}^{1-y} dz \rightarrow \int_0^{1-y} dz$, when the δ functions $\delta(s - \hat{m}_c^2)$ and $\delta(s - \tilde{m}_c^2)$ appear.

References

- [1] S. K. Choi, et al., Phys. Rev. Lett. **91**, 262001 (2003).
- [2] C. Patrignani, et al., Chin. Phys. C **40**, 100001 (2016).
- [3] R. Aaij, et al., Phys. Rev. Lett. **115**, 072001 (2015).
- [4] S. Godfrey and N. Isgur, Phys. Rev. D **32**, 189 (1985).
- [5] M. Voloshin and L. Okun, JETP Lett. **23**, 333 (1976).
- [6] A. De Rujula, H. Georgi and S. L. Glashow, Phys. Rev. Lett. **38**, 317 (1977).
- [7] M. Anselmino, E. Predazzi, S. Ekelin, S. Fredriksson and D. Lichtenberg, Rev. Mod. Phys. **65**, 1199 (1993).
- [8] L. Maiani, F. Piccinini, A. Polosa and V. Riquer, Phys. Rev. D **71**, 014028 (2005).
- [9] R. D. Matheus, S. Narison, M. Nielsen and J. M. Richard, Phys. Rev. D **75**, 014005 (2007).
- [10] F. S. Navarra, M. Nielsen and S. H. Lee, Phys. Lett. B **649**, 166 (2007).
- [11] S. H. Lee, A. Mihara, F. S. Navarra and M. Nielsen, Phys. Lett. B **661**, 28 (2008).
- [12] R. M. Albuquerque and M. Nielsen, Nucl. Phys. A **815**, 53 (2009).
- [13] Z. G. Wang, Eur. Phys. J. C **59**, 675 (2009).
- [14] Z. G. Wang, Eur. Phys. J. C **62**, 375 (2009).
- [15] W. Chen and S. L. Zhu, Phys. Rev. D **83**, 034010 (2011).
- [16] J. R. Zhang and M. Q. Huang, Phys. Rev. D **83**, 036005 (2011).
- [17] C. F. Qiao and L. Tang, Eur. Phys. J. C **74**, 2810 (2014).
- [18] J. R. Zhang, J. L. Zou and J. Y. Wu, Chin. Phys. C **42**, 043101 (2018).

- [19] H. Sundu, S. S. Agaev and K. Azizi, Phys. Rev. D **97**, 054001 (2018).
- [20] R. L. Jaffe and F. Wilczek, Phys. Rev. Lett. **91**, 232003 (2003).
- [21] R. Lebed, Phys. Lett. B **749**, 454 (2015).
- [22] L. Maiani, A. Polosa and V. Riquer, Phys. Lett. B **749**, 289 (2015).
- [23] V. V. Anisovich, M. A. Matveev, J. Nyiri, A. V. Sarantsev and A. N. Semenova, arXiv:1507.07652.
- [24] H. X. Chen, W. Chen, X. Liu, T. G. Steele and S. L. Zhu, Phys. Rev. Lett. **115**, 172001 (2015).
- [25] G. N. Li, M. He and X. G. He, JHEP **12**, 128 (2015).
- [26] Z. G. Wang, Nucl. Phys. B **913**, 163 (2016).
- [27] Z. G. Wang and T. Huang, Eur. Phys. J. C **76**, 43 (2016).
- [28] Z. G. Wang, Eur. Phys. J. C **76**, 70 (2016).
- [29] S. S. Agaev, K. Azizi and H. Sundu, Eur. Phys. J. C **77**, 321 (2017).
- [30] M. Voloshin, Prog. Part. Nucl. Phys. **61**, 455 (2008).
- [31] S. Dubynskiy, M. Voloshin, Phys. Lett. B **666**, 344 (2008).
- [32] R. F. Lebed, R. E. Mitchell and E. S. Swanson, Prog. Part. Nucl. Phys. **93**, 143 (2017).
- [33] H. X. Chen, W. Chen, X. Liu and S. L. Zhu, Phys. Rept. **639**, 1 (2016).
- [34] Z. Y. Di, Z. G. Wang, J. X. Zhang and G. L. Yu, Commun. Theor. Phys. **69**, 191 (2018).
- [35] Z. G. Wang, Eur. Phys. J. C **74**, 2874 (2014).
- [36] Z. G. Wang and T. Huang, Phys. Rev. D **89**, 054019 (2014).
- [37] Z. G. Wang, Eur. Phys. J. C **77**, 174 (2017).
- [38] L. J. Reinders, H. Rubinstein and S. Yazaki, Phys. Rept. **127**, 1 (1985).
- [39] M. A. Shifman, A. I. Vainshtein and V. I. Zakharov, Nucl. Phys. B **147**, 385 (1979).
- [40] P. Colangelo and A. Khodjamirian, At the Frontier of Particle Physics: Handbook of QCD, Vol. **3**, ed. M. Shifman (World Scientific, 2001), pp. 1495.
- [41] L. Maiani, F. Piccinini, A. D. Polosa and V. Riquer, Phys. Rev. D **89**, 114010 (2014).
- [42] M. Nielsen and F. S. Navarra, Mod. Phys. Lett. A **29**, 1430005 (2014).
- [43] Z. G. Wang, Commun. Theor. Phys. **63**, 325 (2015).
- [44] S. S. Agaev, K. Azizi and H. Sundu, Phys. Rev. D **96**, 034026 (2017).
- [45] Z. G. Wang, Eur. Phys. J. C **77**, 78 (2017).
- [46] Z. G. Wang, Commun. Theor. Phys. **63**, 466 (2015).
- [47] Z. G. Wang and Y. F. Tian, Int. J. Mod. Phys. A **30**, 1550004 (2015).
- [48] Z. G. Wang and T. Huang, Eur. Phys. J. C **74**, 2891 (2014).
- [49] Z. G. Wang, Eur. Phys. J. C **74**, 2963 (2014).
- [50] Z. G. Wang, Mod. Phys. Lett. A **29**, 1450207 (2014).